

CO-CONTINUOUS PHASE NANOFIBER COMPOSITES

Christopher C. Bowland, Eric M. Burgeson, Amit K. Naskar
Oak Ridge National Laboratory
1 Bethel Valley Road
Oak Ridge, TN 37831

ABSTRACT

We report on the development of a co-continuous phase composite with a polyacrylonitrile (PAN) nanofiber network integrated into an acrylonitrile-butadiene-styrene (ABS) matrix that offers improved mechanical strength. Homogeneous dispersion of nanomaterials in a matrix can be challenging and typically involves mechanical mixing or chemical modification. This work overcomes this obstacle by taking an inverse approach in that a nanoscale network is synthesized then infiltrated with polymer instead of attempting to disperse the nanomaterial in the polymer. This not only enables excellent homogeneity but also allows the nanoscale phase to be continuous throughout the composite. Here, PAN is electrospun to form a random network of nanofibers having diameters of roughly 200 nm, which is then infiltrated with ABS using solution processing. By optimizing the heat treatments and ABS concentrations, the tensile strength and elastic modulus were improved by 208% and 313%, respectively, as compared to the bare PAN nanofibers. Since there has been significant previous research efforts on electrospinning polymers, many different nanofiber and polymer systems can be made into composites using the methodology established in this work. Therefore, this research offers a new route to create a co-continuous composite with the aim to replace some existing fiber reinforced composites.

1. INTRODUCTION

Nanocomposites have attracted significant research interest due to their ability to significantly alter the mechanical performance of the pristine matrix material.¹⁻³ A challenge remains with dispersing nanomaterials throughout matrices. The approaches typically pursued are physical mixing of the matrix and nanomaterials with optional chemical modification of the materials to create homogeneous dispersions. Our approach here differs in that we create a nanostructured, continuous network prior to matrix infiltration, achieved using a solution-based approach. This creates a co-continuous nanocomposite without requiring additional chemical modification or mechanical mixing. These co-continuous structures have significant mechanical benefits over discrete 2D nanoscale architectures.

Previous nanocomposites have focused on introducing carbon nanotubes^{4, 5}, graphene⁶, nanoclay⁷, nanocellulose^{8, 9}, and ceramic nanoparticles¹⁰⁻¹² into different matrices to enhance mechanical performance. These have mainly focused on physical mixing approaches or chemical modification of the materials to homogeneously disperse the nanomaterials. In particular, nanoparticle and/or matrix functionalization can enhance the filler-matrix interface thus reducing

This manuscript has been authored by UT-Battelle, LLC under Contract No. DE-AC05-00OR22725 with the U.S. Department of Energy. The United States Government retains and the publisher, by accepting the article for publication, acknowledges that the United States Government retains a non-exclusive, paid-up, irrevocable, worldwide license to publish or reproduce the published form of this manuscript, or allow others to do so, for United States Government purposes. The Department of Energy will provide public access to these results of federally sponsored research in accordance with the DOE Public Access Plan (<http://energy.gov/downloads/doe-public-access-plan>).

agglomeration during mixing^{2, 13, 14}. In addition to simply creating a homogeneous dispersion of nanomaterials in the matrix, Naskar et al. indicated in a recent perspective article that having co-continuous phases are advantageous for mechanical properties.¹⁵ This was demonstrated by research on a co-continuous network formed in a thermoplastic consisting of nitrile rubber and lignin.¹⁶ This networking during blending was taken one step further by introducing salt to the mixing procedure to modify domain size and dispersion within the nitrile rubber and lignin blend to create an ionomer.¹⁷

As opposed to these mechanical mixing and chemical modification approaches, this research offers a different approach that aims to create the nanoscale connected network prior to matrix infiltration. The technique used to create these nanosized polymer networks is electrospinning due in part to vast amount of research that has already been performed to develop methods to electrospin nanoscale materials from polymers to ceramics.¹⁸⁻²⁰ This technique involves ejecting a polymer solution from a spinneret, usually just a metal needle with a syringe, and using a high electric potential to collect nanofibers on a grounded substrate. While electrospun materials have not traditionally been thought of as a commercially scalable technique, electrospun materials in the form of mats are now being commercially produced, such as for air filters. Therefore, this paper sets the groundwork for expanding to other material systems that have been achieved through electrospinning and opens the possibility to create co-continuous nanocomposites from various material systems that could not be achieved by simple mechanical mixing and chemical modification.

2. EXPERIMENTATION

2.1 Electrospinning

To make the solution for electrospinning, polyacrylonitrile (PAN) powder was mixed with dimethylformamide (DMF) in a concentration of 4 to 8 wt% PAN and stirred at 70 °C until homogeneous. The PAN used was a copolymer of 95.36 mol% acrylonitrile and 4.64 mol% methyl acrylate (MA). The PAN-MA polymer had a molecular weight M_n 126 kDa and dispersity D_M 2.23. The solution was loaded into a 20 mL syringe (Air-Tite™ All-Plastic Norm-Ject™) with a 304 stainless steel Luer Lock blunt-tipped needle. The metal needle was attached to the positive terminal of a high voltage DC power supply with the ground terminal attached to a rotating metal collection drum. The spacing between the needle tip and collection drum was 14 cm. A syringe pump was used to flow the solution at a rate of between 0.5 and 3 mL/hr with an electric potential between 10 and 20 kV.

Scanning electron microscopy (SEM, Hitachi S4800) was used to evaluate the nanofiber quality and calculate the nanofiber diameters. The nanofibers were coated with 5 nm of gold and the SEM was operated at 10 kV and 10 μ A.

2.2 Composite Fabrication

Solutions of ABS were made by dissolving ABS in acetone at 55 °C for 3-5 days. The ABS was grade GP22-ABS-NT from M. Holland. The electrospun PAN-MA mats were mounted on a rectangular frame to keep the mats under tension during dip coating. The mats were placed in the ABS and acetone solution for several seconds then removed and allowed to dry at room temperature. These mats were then removed from the frame and placed between two steel plates

in the oven set to between 200 and 260 °C for 30 minutes. The steel plates applied a pressure of roughly 2 kPa. This method allowed the PAN-MA nanofibers to remain in tension to prevent it from relaxing and degrading in mechanical properties.

2.3 Mechanical Testing

Prepared composite sheets were sectioned and mechanically tested using an electromechanical tensile frame (MTS, RT/Alliance) in accordance with ASTM D882. The sample dimensions deviated slightly from the dimensions in the standard due to size constraints on the electrospinning setup. The samples were shortened to 10.16 cm. The samples were on average 120 µm thick and approximately 6 mm wide. At least 5 samples of each composite were tested in accordance with the ASTM standard.

3. RESULTS

This investigation began with studying the electrospinning process of PAN-MA to create a nanostructured mat with fiber diameters between 100 and 300 nm. The PAN-MA differed in molecular weight and copolymer concentration from other studies in the literature regarding electrospinning of PAN, so an initial study was performed to create nanofibers with the desired diameter and consistent quality without any particle formation on the mat.

3.1 Nanofiber Synthesis

It should be noted that two different solvents for the dope were tested, dimethyl sulfoxide (DMSO) and DMF. The vapor pressure of DMSO is not high enough to cause evaporation in the air gap between the needle and the grounded collector. This resulted in PAN remaining saturated with solvent when collected and formed a film instead of nanofibers. To avoid this, DMF was selected due to its higher vapor pressure. Switching to this solvent generated PAN nanofibers.

The initial aim was to create PAN electrospun, nonwoven mats with fiber diameters between 100 and 300 nm. This was achieved by modifying both the electric potential during electrospinning and altering the concentration of PAN-MA in DMF. The first investigation used an 8 wt% PAN-MA in DMF solution and was electrospun into fibers at six different electrical potentials ranging from 10 kV to 20 kV. As seen in Figure 1, the fiber diameters were roughly 600 nm and were not affected by the voltage ranges used. An advantage of increasing the electric potential is the ability to then increase the flow rate of the syringe pump to increase the deposition speed of the electrospun mat.

In order to further reduce the fiber diameter, lower concentrations of PAN-MA in DMF were used. In Figure 2, the PAN-MA concentrations of 8, 6, and 4 wt% were tested, and the diameters clearly decreased as the PAN-MA concentration decreased. The nanofibers from the 4 wt% PAN-MA solution were within the desirable diameter range that was determined at the onset of this research.

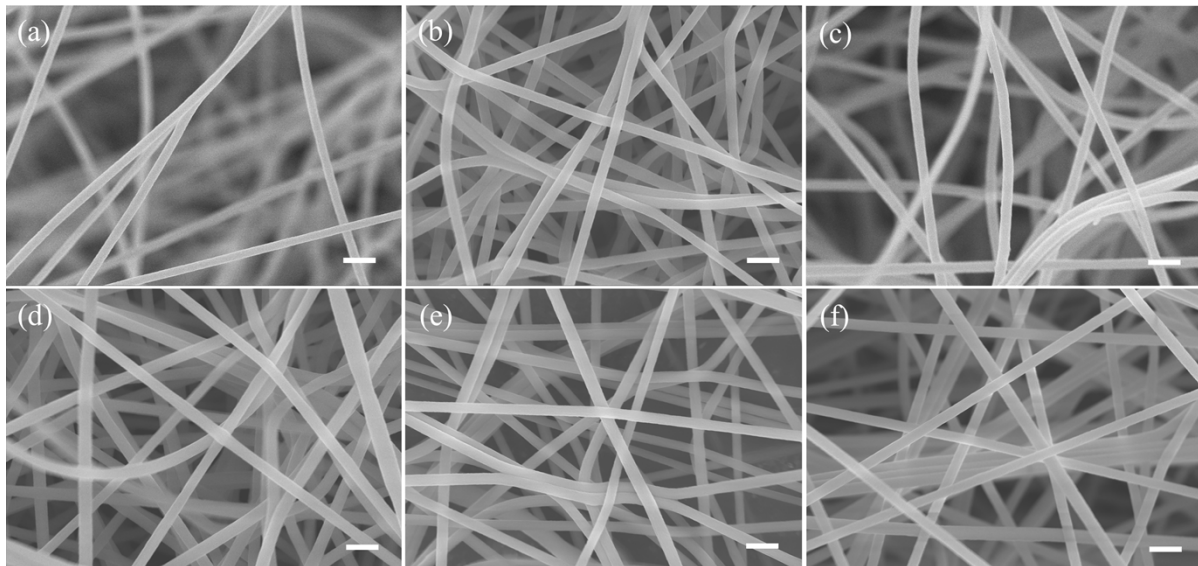


Figure 1. SEM images of electrospun PAN using a 8 wt% PAN concentration in DMF spun at electric potentials of (a) 10 kV, (b) 12 kV, (c) 14 kV, (d) 15 kV, (e) 18 kV and (f) 20 kV. All scale bars are 2 μ m.

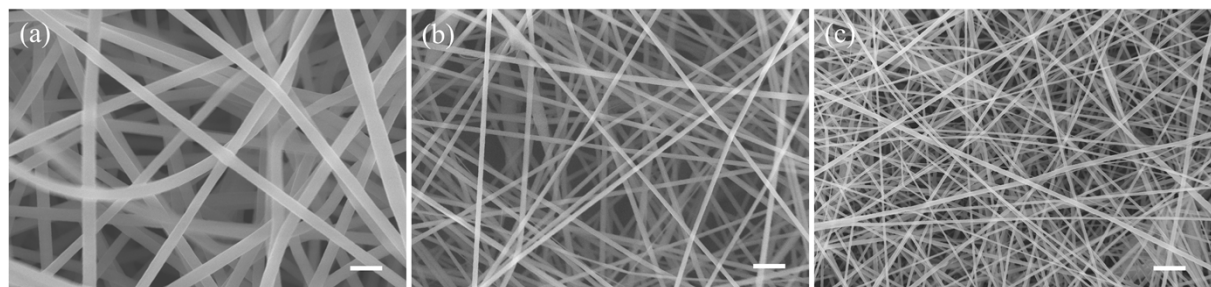


Figure 2. SEM images of electrospun PAN at 15 kV using a PAN concentration of (a) 8 wt%, (b) 6 wt% and (c) 4 wt% in DMF. All scale bars are 2 μ m.

One further test that was performed was increasing the flow rate of the syringe pump to maximize the nanofiber deposition rate. The trick is getting a balance of the flow rate and the electric potential so that a droplet is continuously present at the needle tip to form a Taylor cone. Based on this test, the flow rate was increased from the original rate of 0.5 mL/hr to 3.0 mL/hr. To get a stable dope droplet at the needle tip at the increased flow rate, the viscosity needed to be increased slightly so the PAN-MA concentration was increase to 5 wt%. The resulting fibers can be seen in Figure 3. The average diameter of the 5 wt% PAN-MA nanofibers is 238.5 nm, which was still within the desirable diameter range. This flow rate enabled a sufficiently thick mat of nanofibers to be deposited in 3 hours.

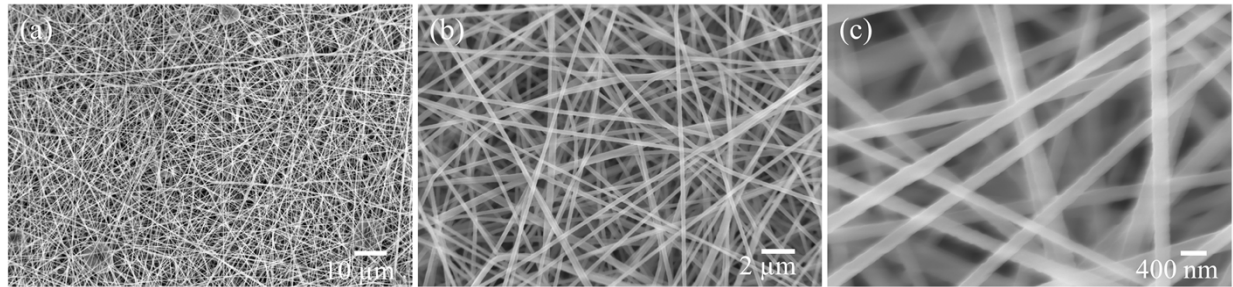


Figure 3. SEM images of electrospun PAN-MA using a dope concentration of 5 wt% PAN-MA and electrospun at 18 kV at a flow rate of 3mL/hr.

3.2 Composite Performance

Upon determining the proper electrospinning parameters, the next step was to infiltrate the nonwoven mats with an ABS matrix. This was achieved by dissolving ABS in acetone with concentrations of 5 wt%, 10 wt%, and 15 wt% ABS. The nanofiber mats were dipped in these solutions then allowed to dry at room temperature. The resulting composite can be seen in the SEM image in Figure 4. The top view of the composites clearly show that the ABS adheres well to the PAN-MA nanofibers and has homogeneous dispersion across the surface, and the cross-sectional image shows that the ABS completely penetrates the nanofiber mat. However, the composite does not have a co-continuous structure since the matrix is not connected throughout the nanofiber scaffold. Nonetheless, tensile tests were performed on these composites with the averages shown in Figure 5. As a baseline, the PAN-MA nanofiber mat with no matrix showed a tensile strength of 8.12 MPa and an elastic modulus of 0.42 GPa while the ABS sheet formed by hot pressing ABS pellets showed a tensile strength of 16.5 MPa and an elastic modulus of 1.07 GPa. After infiltrating the PAN-MA nanofibers with ABS, the tensile strengths were only 7.00 MPa, 11.78 MPa, and 8.80 MPa for the 5 wt%, 10 wt%, and 15 wt% ABS solutions, respectively. These samples also revealed elastic modulus values of 0.45 GPa, 1.48 GPa, and 0.63 GPa for the 5 wt%, 10 wt%, and 15 wt% ABS solutions, respectively. Therefore, it was observed that the tensile strength decreased to below even the PAN nanofibers only sample when the nanofibers were infiltrated with the 5 wt% solution. This may be due to the ABS creating a larger bulk composite structure as compared to the bare nanofibers, and this was a porous structure as observed in Figure 4 thus leading to a decrease in the tensile strength. Despite the tensile strength decreasing, the elastic modulus of the 5 wt% sample was similar to the bare nanofibers. This suggests that the ABS was not connected throughout the nanofiber network thus giving the composite the modulus of just the PAN nanofibers. The 10 wt% sample saw an increase in both tensile strength and elastic modulus as compared to the 5 wt% sample. However, further increasing the ABS concentration to 15 wt% decreased the mechanical properties. Overall, all the composites showed lower tensile strengths as compared to the ABS only samples. The low tensile values may be due in part to the porous structure observed in the SEM images in Figure 4. To create a co-continuous structure and increase the performance of the composite, hot pressing procedures were performed.

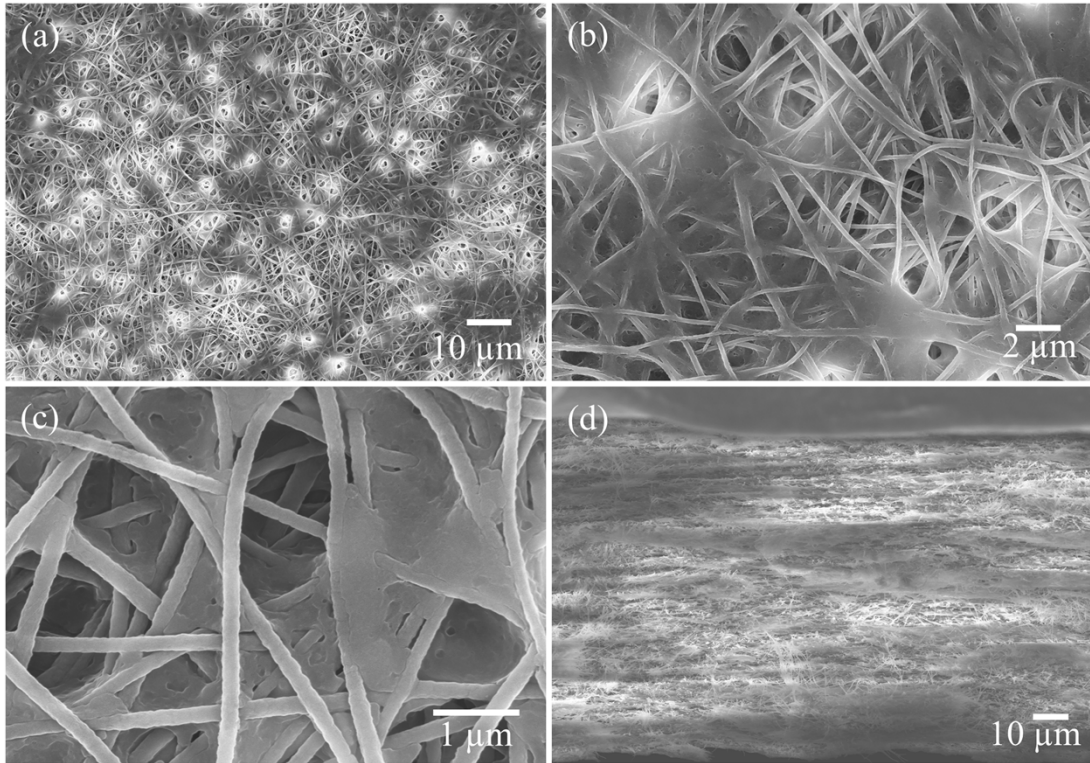


Figure 4. SEM images of the electrospun nanofibers after dip coated in the 5 wt% ABS in acetone solution and dried. (a)-(c) Show the top surface of the composite and (d) is the cross-section of the nanocomposite.

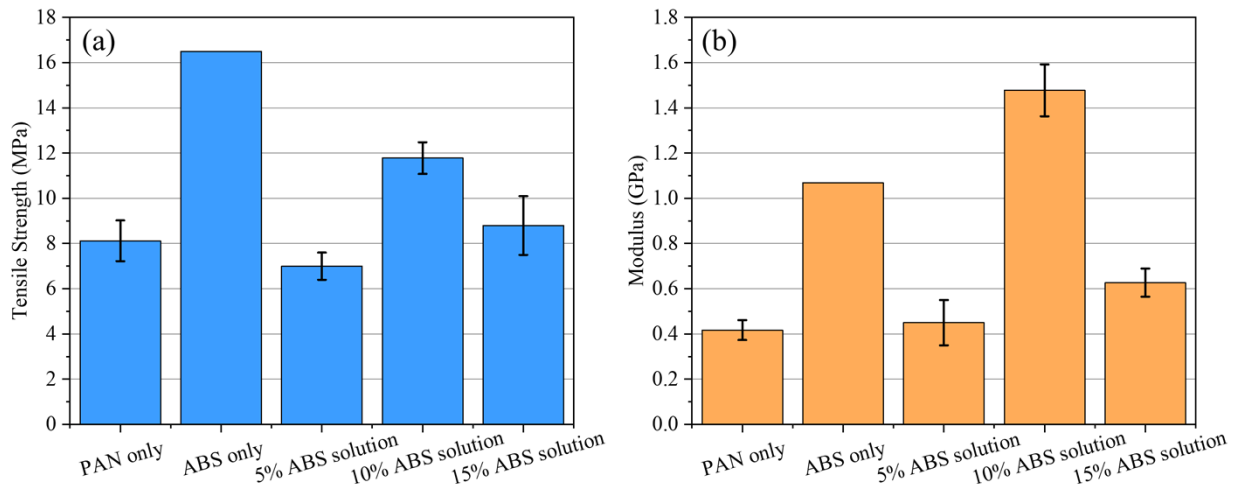


Figure 5. Tensile tests showing the (a) tensile strength and (b) elastic modulus of the PAN nanofibers without an ABS matrix, the ABS only, and the PAN nanofibers in the ABS matrix using three different ABS concentrations. These were all performed before pressing the samples at elevated temperatures. The error bars represent one standard deviation.

Hot pressing was performed at 210, 220, 230, 240 and 260 °C for 30 minutes. This procedure served multiple functions. It helped densify the composite and create a continuous ABS network. At these temperatures, the PAN-MA begins its stabilization process which involves oxidation and cyclization of the polymer. With the ABS coating most of the nanofibers, they were most

likely starved of oxygen thus constricting the stabilization process to just cyclization. By cyclizing the PAN-MA nanofibers with the ABS coating them, it was hypothesized that the acrylonitrile portion of ABS may partially cyclize with the PAN-MA thus enhancing the bonding between the matrix and the nanofibers. This may be the reason for the sharp increase in both tensile strength and elastic modulus observed at 220 °C as seen in Figure 6. For example, the 5 wt% ABS solution sample increased its tensile strength from 15.6 MPa to 47.4 MPa when increasing the hot pressing temperature from 210 to 220 °C. Despite this promising result of significantly increasing the mechanical performance of the composites as a function of hot pressing temperature, increasing the hot press temperature above 220 °C has a negative effect on the mechanical properties. However, the PAN-MA only sample saw an increase in mechanical performance as a function of increasing. This sample was not hot pressed though. It was heat treated in air, which allowed it to both cyclize and oxidize. The increase in strength of the PAN-MA only sample was not translated to the strength of the composite. Overall, it was shown that there was an optimum hot pressing temperature of 220 °C that showed significant tensile strength and elastic modulus increases for all concentrations of ABS.

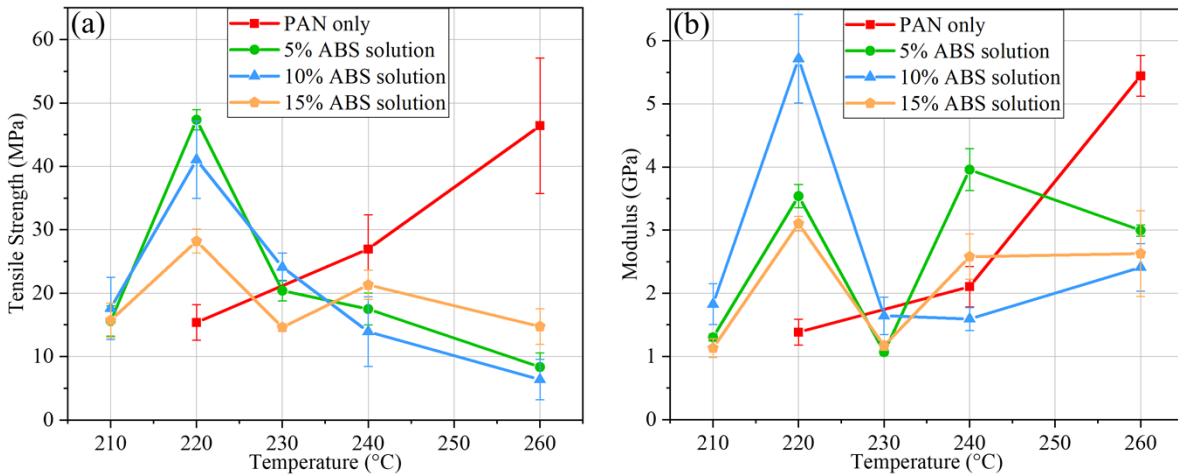


Figure 6. The (a) tensile strength and (b) elastic modulus of composites coated with different concentrations of ABS and hot pressed at various temperatures. The error bars represent one standard deviation.

4. CONCLUSIONS

An initial study was performed on the electrospinning of the PAN-MA to determine the proper electrospinning conditions. The resulting conditions were a dope with 5 wt% PAN-MA in DMF with a flow rate of 3.0 mL/hr and an electrical potential of 18 kV over a 14 cm air gap. These conditions produced fibers with an average diameter of 238.5 nm. It was shown that infiltrating these nanofibers with ABS using a solution-based technique did not necessarily increase the overall strength of the composites. The composites had to be hot pressed in order to experience significant strength enhancements. An optimum hot pressing temperature of 220 °C was observed where the highest tensile strength was 47.4 MPa for the 5 wt% ABS solution sample and the highest elastic modulus was 5.71 GPa for the 10 wt% ABS solution sample. The enhanced tensile strength equates to a 208% improvement and 187% improvement as compared to the bare nanofibers at 220 °C and original ABS, respectively. The elastic modulus equates to a 313% increase and 435% over the bare nanofibers at 220 °C and original ABS, respectively. Therefore, this established a route to create a co-continuous nanocomposite with enhanced

mechanical properties that could be easily translated to other material systems by taking advantage of other nanofibers produced using electrospinning.

5. ACKNOWLEDGEMENTS

Research sponsored by the Wigner Fellowship Program as part of the Laboratory Directed Research and Development Program of Oak Ridge National Laboratory, managed by UT-Battelle, LLC, for the U. S. Department of Energy.

6. REFERENCES

- [1] Hussain, F., Okamoto, M., and Gorga, R., "Review article: polymer-matrix nanocomposites, processing, manufacturing, and application: an overview," *Journal of Composite Material* 40(17), 1511-1575 (2006).
- [2] Vaia, R.A. and Giannelis, E.P., "Polymer nanocomposites: status and opportunities," *MRS bulletin* 26(5), 394-401 (2001).
- [3] Sun, L., Gibson, R.F., Gordaninejad, F., and Suhr, J., "Energy absorption capability of nanocomposites: a review," *Composites Science and Technology* 69(14), 2392-2409 (2009).
- [4] Eitan, A., Fisher, F., Andrews, R., Brinson, L., and Schadler, L., "Reinforcement mechanisms in MWCNT-filled polycarbonate," *Composites Science and Technology* 66(9), 1162-1173 (2006).
- [5] Suhr, J. and Koratkar, N.A., "Energy dissipation in carbon nanotube composites: a review," *Journal of Materials Science* 43(13), 4370-4382 (2008).
- [6] Young, R.J., Kinloch, I.A., Gong, L., and Novoselov, K.S., "The mechanics of graphene nanocomposites: a review," *Composites Science and Technology* 72(12), 1459-1476 (2012).
- [7] Lincoln, D., Vaia, R., Wang, Z.-G., and Hsiao, B., "Secondary structure and elevated temperature crystallite morphology of nylon-6/layered silicate nanocomposites," *Polymer* 42(4), 1621-1631 (2001).
- [8] Lee, K.-Y., Aitomäki, Y., Berglund, L.A., Oksman, K., and Bismarck, A., "On the use of nanocellulose as reinforcement in polymer matrix composites," *Composites Science and Technology* 105, 15-27 (2014).
- [9] Dufresne, A., "Nanocellulose: a new ageless bionanomaterial," *Materials Today* 16(6), 220-227 (2013).
- [10] Alamri, H. and Low, I.M., "Characterization of epoxy hybrid composites filled with cellulose fibers and nano-SiC," *Journal of Applied Polymer Science* 126(S1), E221-E231 (2012).
- [11] Ma, J., Mo, M.-S., Du, X.-S., Rosso, P., Friedrich, K., and Kuan, H.-C., "Effect of inorganic nanoparticles on mechanical property, fracture toughness and toughening mechanism of two epoxy systems," *Polymer* 49(16), 3510-3523 (2008).
- [12] Wu, C.L., Zhang, M.Q., Rong, M.Z., and Friedrich, K., "Silica nanoparticles filled polypropylene: effects of particle surface treatment, matrix ductility and particle species on mechanical performance of the composites," *Composites Science and Technology* 65(3), 635-645 (2005).
- [13] Zhao, Y., Thorkelsson, K., Mastroianni, A.J., Schilling, T., Luther, J.M., Rancatore, B.J., Matsunaga, K., Jinnai, H., Wu, Y., and Poulsen, D., "Small-molecule-directed

nanoparticle assembly towards stimuli-responsive nanocomposites," *Nature materials* 8(12), 979 (2009).

- [14] Stefk, M., Mahajan, S., Sai, H., Epps III, T.H., Bates, F.S., Gruner, S.M., DiSalvo, F.J., and Wiesner, U., "Ordered three-and five-ply nanocomposites from ABC block terpolymer microphase separation with niobia and aluminosilicate sols," *Chemistry of Materials* 21(22), 5466-5473 (2009).
- [15] Naskar, A.K., Keum, J.K., and Boeman, R.G., "Polymer matrix nanocomposites for automotive structural components," *Nature nanotechnology* 11(12), 1026-1030 (2016).
- [16] Tran, C.D., Chen, J., Keum, J.K., and Naskar, A.K., "A new class of renewable thermoplastics with extraordinary performance from nanostructured lignin-elastomers," *Advanced Functional Materials* 26(16), 2677-2685 (2016).
- [17] Barnes, S.H., Goswami, M., Nguyen, N.A., Keum, J.K., Bowland, C.C., Chen, J., and Naskar, A.K., "An Ionomeric Renewable Thermoplastic from Lignin-Reinforced Rubber," *Macromolecular rapid communications*, 1900059 (2019).
- [18] Huang, Z.-M., Zhang, Y.-Z., Kotaki, M., and Ramakrishna, S., "A review on polymer nanofibers by electrospinning and their applications in nanocomposites," *Composites science and technology* 63(15), 2223-2253 (2003).
- [19] Ramaseshan, R., Sundarrajan, S., Jose, R., and Ramakrishna, S., "Nanostructured ceramics by electrospinning," *Journal of Applied Physics* 102(11), 111101 (2007).
- [20] Li, D., McCann, J.T., Xia, Y., and Marquez, M., "Electrospinning: a simple and versatile technique for producing ceramic nanofibers and nanotubes," *Journal of the American Ceramic Society* 89(6), 1861-1869 (2006).